A low-cost indoor real time locating system based on TDOA estimation of UWB pulse sequences

A low-cost indoor real time locating system based on TDOA estimation of UWB pulse sequences

Stefano Bottigliero, Daniele Milanesio, Maurice Saccani, Riccardo Maggiora

***Abstract*—One of the most popular technology adopted for indoor localization is Ultra Wideband Impulse Radio (IR-UWB). Thanks to its peculiar characteristics, it is able to overcome the multipath effect that severely reduce the capability of receivers (sensors) to estimate the position of trasmitters (tags) in complex environments. In this paper we introduce a new low cost Real Time Locating System (RTLS) that does not require time synchronization among sensors and uses a one-way communication scheme to reduce the cost and complexity of tags. The system is able to evaluate the position of a large number of tags by computing the Time Difference of Arrival (TDOA) of UWB pulse sequences received by at least three sensors. In the presented system, the tags transmit sequences of 2 ns UWB pulses with carrier frequency of 7.25 GHz. Each sensor processes the received sequences with a two steps correlation analysis performed firstly on a Field Programmable Gate Array (FPGA) chip and successively on an on-board processor. The result of the analysis is the Time Of Arrival (TOA) of the tag sequence at each sensor and the ID of the associated tag. The results are sent to an host PC implementing trilateration algorithm based on the TDOA computed among sensors. We will describe the characteristics of the custom hardware that has been designed for this project (tag and sensor) as well as the processing steps implemented that allowed us to achieve an optimum localization accuracy of 10 centimeters.**

***Index Terms*—Indoor Positioning, Ultra Wideband (UWB), Time Difference of Arrival (TDOA), localization, low cost.**

I. Introduction

ULTRA-Wideband Impulse Radio (IR-UWB) is an important contendant among the indoor localization technologies. The very short duration of the pulses grants it robustness against multipath interference that affect the ranging accuracy [1] [2].

In UWB positioning systems, it is common to use Time Of Arrival (TOA), Time Of Flight (TOF), Time Difference of Arrival (TDOA), Angle Of Arrival (AOA) [3] or the Received Signal Strengh Indicator (RSSI) [4] at receivers (sensors) to evaluate the position of transmitters (tags) in an indoor environment. In [5] [6] [7] an overview of localization systems based on these different methods is presented. Time-based approaches like the TOF and TDOA are the optimum choices when the goal is to reach centimeters accuracy [8] [9]. On the market there are already various solution with different time-based approaches such as DecaWave [10], Ubisense [11] and Zebra [12].

The DecaWave DW1000 system uses the two-way ranging (TWR) TOF measurement approach with a ranging accuracy of 10 cm [13] and a typical update rate of 3.5 Hz. The update rate need to be lowered as the number of tags to track increases. Each device can be configured as sensor or tag and, thanks to the TWR approach, does not need a common clock source. Nowadays several commercial solutions like Pozyx [14], TimeDomain [15], Sewio [16], Quantitec [17] and OpenRTLS [18], adopt the DecaWave chipsets.

Some of these systems uses the UWB TWR approach together with the informations coming from an Inertial Measurement Unit (IMU) embedded in the tag that allows to generate useful attitude informations. The fusion of different kinds of location dependent parameters is used in indoor navigation systems under the name of hybrid localization techniques [19]. The performances of this kind of systems are evaluated in [20] [21] [22]. Among them, the position accuracy and sensor performances of the Pozyx commercial solution are evaluated in [23] [24]. Even though systems based on hybrid localization technique allow to achieve 10 cm range accuracy, the higher complexity of the tag hardware increases the overall solution cost.

The Ubisense system adopts the TDOA approach using the time difference information determined between pairs of sensors connected with a timing cable [25]. The system is capable to provide a localization accuracy of 15 cm and an update rate from 0.1 to 20 Hz. The performances of the DecaWave and Ubisense systems are compared in [26].

In [27] a technique that combines TDOA and TOF measurements is proposed. It is based on the DecaWave DW1000 system and, thanks to the combination of the two methods, allows to compensate their respective limitations and increase the localization accuracy in a cooperative scenario [28] [29]. The combination of the two methods can effectively improve the accuracy of the TDOA method alone but requires a more complex architecture.

The Zebra system uses the TDOA approach and is capable to reach 30 cm localization accuracy with a maximum update rate of 200 Hz. The overall cost of the hardware infrastructure and tags is very high compared to the DecaWave and Ubisense systems but allows tracking of a large number of fast moving tags.

In this paper we propose a one-way, UWB RTLS based on TDOA computation using a sensors network where the time synchronization among the sensors is not implemented in a wired network but by means of a reference tag. To adress the issue, a solution where one sensor transmit a synchronization signal immediatly after receiving an impulse signal from a target tag was proposed in [30]. The goal is to design an

The authors are with the Department of Electronics and Telecommunications, Politecnico di Torino, 10129 Torino, Italy (e-mail: stefano.bottigliero@polito.it; daniele.milanesio@polito.it; maurice.saccani@polito.it; riccardo.maggiora@polito.it)

RTLS system with better performances with respect to the system already on the market, designing custom hardware and implementing dedicated software to reduce the overall cost of the system infrastructure.
In the following section II we will introduce our new sensors network solution. In section III we will describe the system infrastructure by describing the prototypes of both the transmitter and the receiver; for both we designed and manufactured custom, low cost hardware. In section IV we discuss the two steps processing performed by the sensor system on chip (SoC) that allows to compute the TOA of the UWB signal and to associate it to the corresponding transmitter. We also present the localization algorithm performed on a dedicated PC application based on the trilateration technique. Finally, in Section V, we will present the experimental results obtained in a realistic, indoor laboratory harsh environment where the measurement setup to evaluate the localization accuracy, resolution and tracking capabilities of the system was installed.

II. Proposed UWB TDOA based solution

For the RTLS system developed in this project, we adopted a localization approach based on TDOA computation. The choice of using a time-based location dependent parameter instead of power-based one like RSSI is associated to the higher accuracy that the time-based parameters allows to achieve [31] [32], that is our main goal together with overall system cost reduction. To compute the position of a target tag, it is necessary to evaluate its distance with respect to a number of Sensors located in known position. In a 2D TDOA RTLS system a minimum of three sensors is required. The main disadvantage of the TDOA architecture is that the sensors require a common time base to synchronize the measurements. The synchronization clock must comply to very stringent requirements of stability, speed and connection over the sensors network. These requirements cause this solution to be extremely cost inefficient. To overcome this issue we adopt a different architecture that does not require a common clock among the sensors but instead, uses a reference tag, placed in a known fixed position like proposed in [33].
In this configuration each sensor has its independent clock and, by comparing the TOA measures with respect to the ones coming from the reference tag, it is capable to compensate the time offset among the sensor clocks (see Figure 1).
The algorithm that computes the tag's position is based on the multilateration of the signal transmitted by the tag and received by the sensors. In order to work properly, it requires to know the TDOA among the sensors (in an ideal case a minimum of three sensor are synched using the same clock signal). We define as $T_i^{Sx}(N)$ the TOA of a sequence from a generic tag T_i arriving at the sensor Sx at instante of time N. The algorithm performing the TDOA computes the time differences between the reference sensor (S1) and the slave sensors (S2 and S3) as:

$$TDOA_{12} = T_i^{S1}(N) - T_i^{S2}(N) \tag{1}$$

$$TDOA_{13} = T_i^{S1}(N) - T_i^{S3}(N) \tag{2}$$

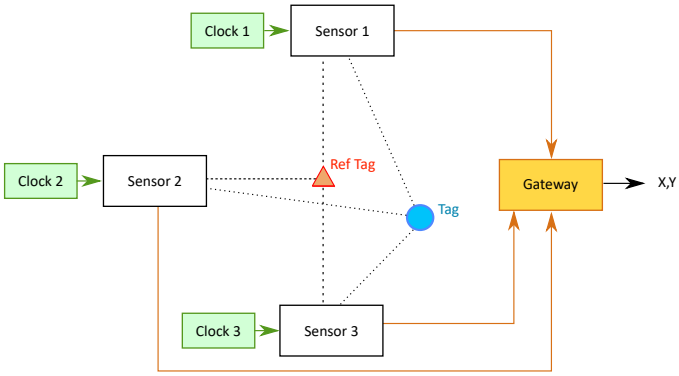

Fig. 1. High level block diagram of an RTLS system based on TDOA measurements with the use of a Reference Tag in fixed position.

Having the TDOA, it is sufficient to convert them into distances and use them together with the known positions of each sensor in the multilateration formula [34] [35] [36]. The results are the bidimensional coordinates of the tag's position. Since the sensors are not synched using the same clock signal, we need to compensate the frequency and time differences among the individual sensor clocks using the reference tag.
The distance between the sensors and the reference tag translates into an offset representing the time difference between the sensors and the reference tag and it is equal to:

$$off_{12} = \frac{(d_{T_{Ref}S1} - d_{T_{Ref}S2})}{c} \tag{3}$$

$$off_{13} = \frac{(d_{T_{Ref}S1} - d_{T_{Ref}S3})}{c} \tag{4}$$

Where $d_{T_{Ref}Sx}$ is the distance between the reference tag and sensor x and c is the speed of light. Furthermore, all TOA measurements must be referred to those associated to the reference tag, compensating the clock's time differences. To compensate the frequency difference we multiply the TDOA by a correction factor called "SRF_{xy}" that relates all the differences measurements to the ratio between the Sequence Repetition Frequency (SRF) of the reference tag computed at the reference sensor, and the SRF of the reference tag computed at the slave sensors:

$$SRF_{12} = \frac{SRF^{S1}_{T_{Ref}}}{SRF^{S2}_{T_{Ref}}} = \frac{T^{S1}_{Ref}(N) - T^{S1}_{Ref}(N-1)}{T^{S2}_{Ref}(N) - T^{S2}_{Ref}(N-1)} \tag{5}$$

$$SRF_{13} = \frac{SRF^{S1}_{T_{Ref}}}{SRF^{S3}_{T_{Ref}}} = \frac{T^{S1}_{Ref}(N) - T^{S1}_{Ref}(N-1)}{T^{S3}_{Ref}(N) - T^{S3}_{Ref}(N-1)} \tag{6}$$

Where $SRF^{S1}_{T_{Ref}}$ is the sequence repetition frequency of the reference tag evaluated at the reference sensor and $SRF^{S2,3}_{T_{Ref}}$ is the sequence repetition frequency of the reference tag at sensor 2 or 3. The TDOA equation then becomes :

$$\begin{aligned} TDOA_{12} &= (T_i^{S1}(N) - T_{ref}^{S1}(N)) \\ &\quad - (T_i^{S2}(N) - T_{ref}^{S2}(N) - off_{12}) \cdot SRF_{12} \end{aligned} \tag{7}$$

$$\begin{aligned} TDOA_{13} &= (T_i^{S1}(N) - T_{ref}^{S1}(N)) \\ &\quad - (T_i^{S3}(N) - T_{ref}^{S3}(N) - off_{13}) \cdot SRF_{13} \end{aligned} \tag{8}$$

The sensors can sometimes miss a sequence due to obstacles or occlusions in the line of sight (LOS). The host application must be able to recognize when a sequence has been missed and to discard the TDOA computation for the three sensors. Knowing that the TDOA between the same sequence at different sensors cannot be larger than the propagation time between the sensors, the software considers only groups of TDOA smaller than the maximum propagation time considered in the scenario. Only when a correct group of TDOA is calculated the software validates the localization.

To avoid ambiguity in the association of a target sequence with the reference one it is sufficient to have the SRF of the reference tag slightly different from that of the target tag, in this way there will be a net difference between the results corresponding to a correct time association and a wrong one. The carrier frequency is modulated using On Off Keying (OOK) coding, when a bit is equal to "1" a pulse is transmitted and, when a bit is equal to "0" no pulse is transmitted. This modulation simplifies the tags hardware design dramatically. The transmitted pulse shape is shown in Figure 2, it is a 2 ns pulse with a carrier frequency of 7.25 GHz. The duration of the inter pulse period is 50 ns, corresponding to a pulse repetition frequency of 20 MHz. The time duration of the pulse inside the period corresponds to a duty cycle of $D = 4\%$. This very low value of D allows the tag to require very low power. The signal transmitted by each tag is a sequence of 15 bits organized as follows:

- The first 7 bits represent the Preamble Sequence of the signal. This part is common to all tags and is used to recognize the presence of a tag's sequence in the received data and to compute the TOA;
- The remaining 8 bits represent the tag ID Sequence number. This second part is unique to each tag and is used to associate the TOA to the specific tag.

While the tag ID can assume any possible value obtainable by the combination of 8 bits, the preamble takes the specific behavior of a Barker code [37]. We use a modified version of Barker code where there is no pulses in correspondance of a $+1$ in the sequence.

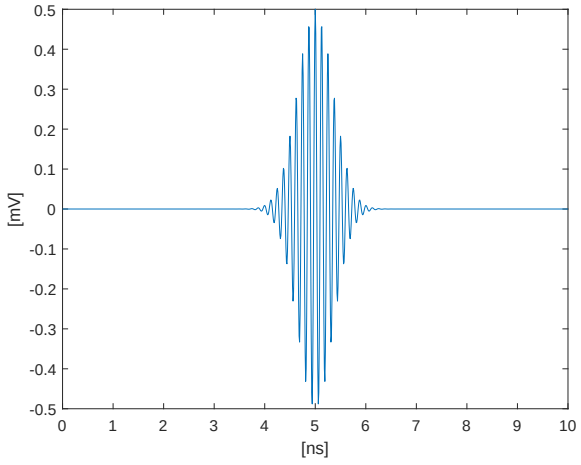

Fig. 2. Shape of the transmitted UWB Pulse.

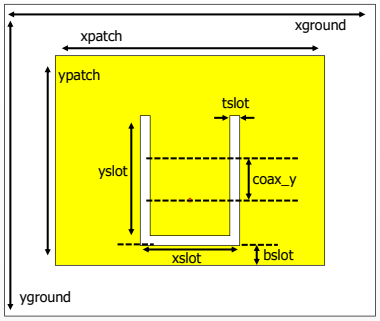

Fig. 3. UWB Receiving Patch antenna.

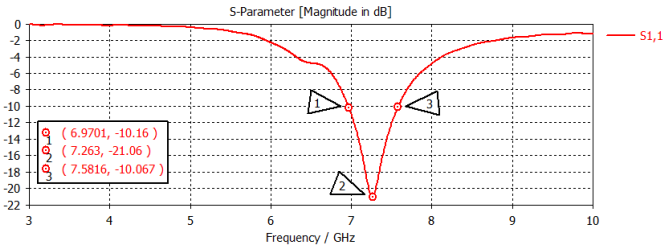

Fig. 4. UWB Receiver Antenna S11.

III. System Architecture

The UWB sensors market is dominated by commercially very expensive systems [38] very often based on proprietary solutions. Our goal is to design and implement a solution with reduced cost of production with respect to commercially available systems. For this reason, we decided to design our own hardware (and software) for the entire localization system. Our system is made up of a minimum of three sensors receiving the UWB signals, the tags, an ethernet switch to connect all the sensors together in a LAN and a host PC running the localization software. The sensor is assembled connecting two custom boards: the UWB receiver board and the processing board.

A. The UWB Receiver

The UWB receiver, mounted on top of the processing board, picks up the signal using a custom slotted UWB patch antenna and a DC filter. The slotted UWB patch antenna is printed on a 1.6 mm thick FR-4 substrate. In Figure 3 and Table I the geometrical parameters of the patch and the slot used to increase the bandwidth of the antenna are reported. The antenna is vertically polarized.

The slotted patch has an $S_{11} = -21$dB at the central frequency of 7.25 GHz and a bandwidth of $\Delta B = 0.6$ GHz between the two points at -10 dB (see Figure 4). The directivity reach 6 dBi in magnitude and an angular width (at -3 dB) of 97° for both planes at $\phi = 0°$ and $\phi = 90°$. The slotted patch antenna directivity allows to place the sensor in rooms corners maximizing the covered localization area. The antenna is connected to the UWB receiving module using a Sub Miniature A (SMA) connector.

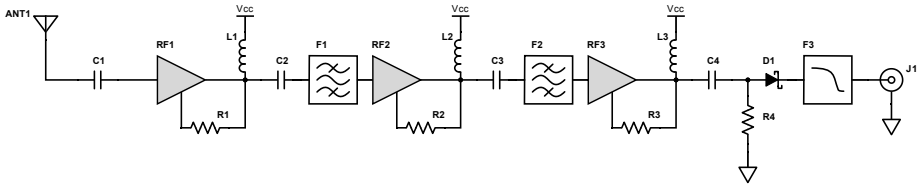

Fig. 5. Custom UWB receiver schematic. The UWB signal is amplified, filtered, rectified and low pass filtered.

TABLE I
PATCH ANTENNA GEOMETRICAL PARAMETERS

Parameter	mm
X Ground	16.4
Y Ground	15.3
X Patch	10
Y Patch	8.9
X Slot	2.0
Y Slot	7.0
Slot Height	0.5
Y Coax	3.0

The shematic of the UWB receiving module is shown in Figure 5. From the antenna, the signal is provided to the first of three cascaded Low Noise Amplifier (LNA) stages. Each amplification stage is designed with a center frequency of 7.25 GHz to have nominal fixed gain of 20 dB with low noise figure, below 1.5 dBm and 5 V single voltage supply compatibility. The selected amplifier chip is the Macom MAAL-011130 [39]. The output of each LNA is connected to a bias tee circuit [40] to provide the RF signal to the next amplification stage while separating it from the voltage supply. After the first amplification stage we filter the signal using a Coupled Line Band Pass Filter (BPF), in microstrip technology, and provide it to a second identical amplification stage. The BPF is designed to have small insertion loss of 1 dB, centered at 7.25 GHz with 500 MHz bandwidth. The second amplification stage is followed by another coupled line BPF identical to the previous one. A third and last amplification stage is present. The theoretical gain of the receiving chain is about 50 dB. The analog amplification chain is dimensioned empirically to correctly receive tag signals up to a maximum distance of 30 m in an open environment. The signal is rectified using a series Schottky diode, provided to an integrated Low Pass Filter (LPF) and the obtained base-band signal is sent to a Sub Miniature Push-on (SMP) connector that connects to the processing board. The UWB receiver board is shown in Figure 6.

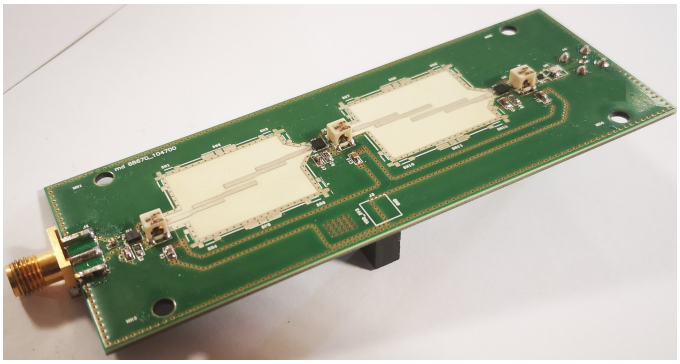

Fig. 6. Custom UWB receiver board.

B. The Sensor processing board

The custom designed processing board gets the signal from the UWB receiver and samples it using the HMCAD1511 analog to digital converter (ADC) from Analog Devices with a sampling frequency of 1 GSps and 8-bit resolution. The 1 GHz differential sampling clock required by the ADC is provided by the ADF4360-7 Phase Locked Loop (PLL) from Analog Devices. The sampled data are sent to a Zynq7000 SoC from Xilinx. This family of SoC offers the advantages of having both FPGA and a dual core ARM processor in the same chip for a very affordable price. The data processing provides the ID of the tag associated to the elaborated sequence and its TOA. These results are sent by each sensor to a host PC throught a local area network (LAN). The board is 12 cm by 12 cm large and is powered using a standard 12V external power supply (see Figure 7).

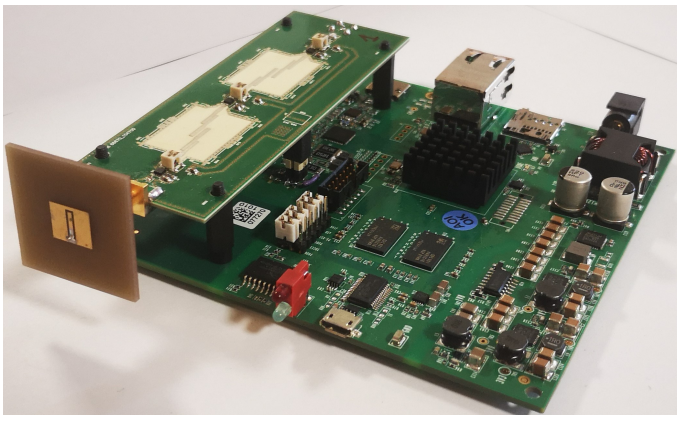

Fig. 7. Top view of the custom sensor board processing board and UWB receiver are connected together.

C. The tag

The tag is the active low-power transmitting device that we want to locate. It is made up of four parts: a custom UWB elliptic dipole antenna; a single transistor RF pulsed

oscillator at the carrier frequency; a digital control circuit to manage the bit sequence characteristics and generate the pulses and a battery. The elliptic dipole antenna design methodology adopted is presented in [41]. This kind of antenna allows to have wideband impedance matching and omnidirectional radiation pattern and it is printed on the same tag board. The tag generates the sequence of 2 ns UWB pulses at the working frequency of 7.25 GHz.
The pulsed oscillator circuit used to generate the signal is identical to the one proposed in [42]. The oscillator is based on a single high frequency transistor in a negative resistance configuration. The oscillation is driven by a 2 ns base-band pulse signal sequence generated by the digital timing circuit. The inter pulse period is fixed to 50 ns (20 MHz) while the Sequence Repetition Frequency (SRF), as well as the tag ID number are hardwired for each tag.
In Figure 8 a top view of the tag is shown; the assembly is 11.5 cm wide, 5.5 cm long and 1.5 cm thick.

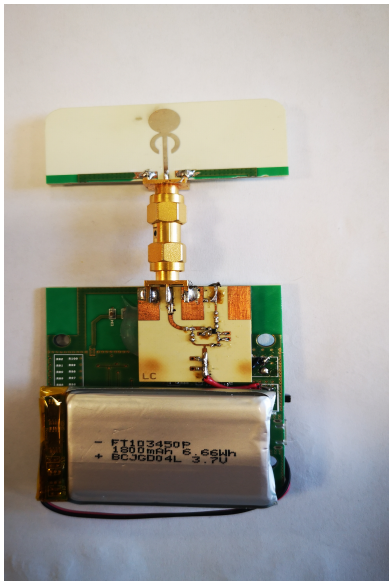

Fig. 8. Top view of the transmitting tag. The digital circuit located below the battery, drives the emitter of the high speed transistor in the RF oscillator to generate the 2 ns pulses.

IV. Software Implementation

The system software is subdivided in three parts: The SoC program, made up of the FPGA code and the ARM processor code, running on each sensor and the User Interface running on a host PC connected to the sensors via LAN.
The FPGA code implements an architecture that receives the data from the ADC, verify the presence of the preamble sequence in the incoming data stream by means of a fast correlation operation, compute a coarse TOA associated to the received data and send this information to the ARM processor. The ARM code further manipulates the information from the FPGA by correlating the received data with the sequences associated to all the possible tags. Once the tag ID is identified, it refines the measure of the TOA previously computed by the FPGA performing an accurate correlation with a ramp shaped reference signal. The ARM is also responsible to implement a superresolution technique to further improve the TOA accuracy.
The obtained TOA and tag ID informations are sent to the host PC running the Graphic User Interface (GUI) application. The GUI receives the data from the sensors, computes the TDOA between the sensors and executes the trilateration algorithm that provides the cartesian coordinates of the tags. The obtained positions and the associated data are plotted on a 2D map for visualisation.

A. FPGA Processing

The FPGA analyzes the data from the ADC and correlates them with the preamble sequence to verify the presence of a tag sequence and to perform a coarse measure of the TOA as shown in Figure 9. The incoming data are provided to a custom block, the correlator, that is the processing core of the whole FPGA design. It performs the correlation between the data and the preamble sequence, saves the results into a buffer, and provides the results to the threshold block. If one of the correlation results is higher than a threshold, it means that a preamble sequence has been found in the data stream, and it saves the data into a buffer and sends them to the ARM processor. The value of a timer representing the coarse TOA of the recognized sequence is associated to the buffered data. The coarseness is related to the period (equal to 8 ns) of the processing clock necessary to elaborate the data coming from the ADC in real time. The TOA will be refined by the ARM processor software down to the sampling clock time resolution of 1 ns.

The FPGA correlation is performed multiplying the data stream coming from the ADC with a vector of data called Symbol Mask that has the same shape as a single transmitted base-band pulse in the sequence. The correlation result is computed as:

$$Del[i] = \sum_{j=0}^{49} ADC\_Data[j] \cdot Symbol\_Mask[j] \qquad (9)$$

where $Del[i]$ is the i-th correlation result while $ADC\_Data[j]$ and $Symbol\_Mask[j]$ are respectively the sampled data in position k of the received data buffer and the corresponding symbol mask bit as shown in Figure 10. The pulses in the sequence are separated by an interval of 50 nanoseconds: since the sampling frequency is 1 GHz, each pulse lasts for 50 samples, forcing the symbol mask to be that long as well.
At each 125 MHz clock cycle, the FPGA receives eigth new data from the ADC to be correlated. The FPGA correlation block saves the new data in a buffer and elaborate them in parallel providing eight correlation values. The multiplication between the data buffer and the symbol mask is istantiated eigth times, one for each new received sample and, for each instance, the data buffer is shifted by one position. For each instance, the result of the multiplications are added together to obtain the correlation values that are saved in a buffer (see Figure 10). The goal is to recognize the preamble sequence in the incoming data stream. We take advantage of the fact that each symbol in the sequence has a fixed length of 50

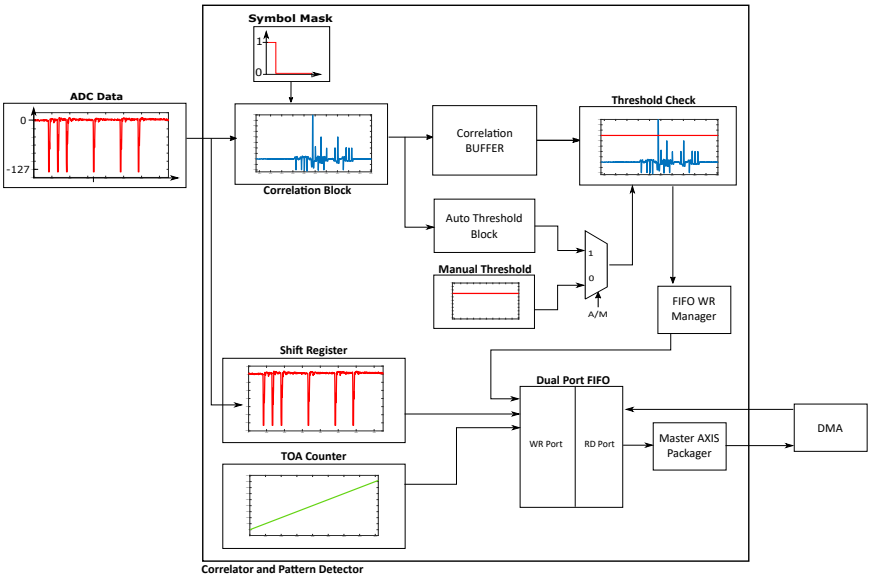

Fig. 9. High level block diagram of the processing steps performed in FPGA starting from the correlation of the incoming data with the symbol mask, to the thresholding operation to the final storage in the data buffer.

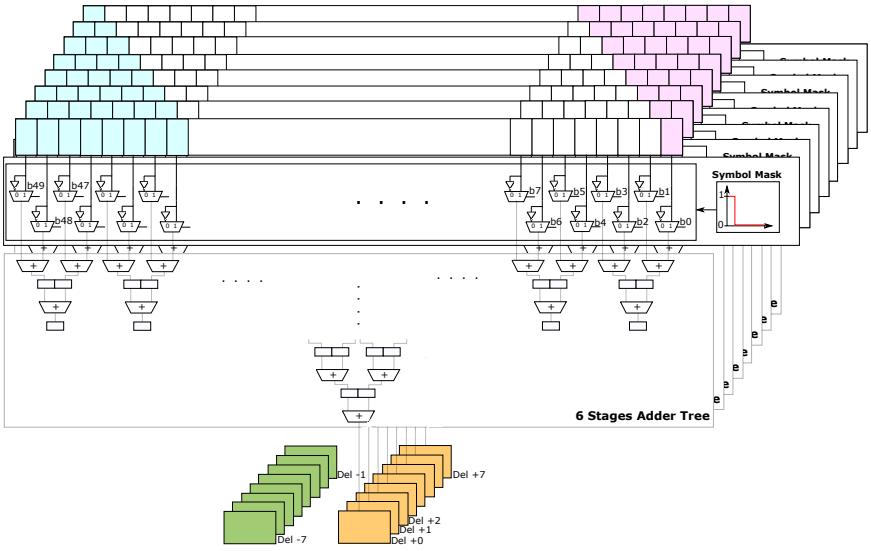

Fig. 10. Block diagram of the correlator block. It shows the eight instantiations of the elaboration blocks that compute the correlation delays and the final buffer where all the correlation results are stored. Each clock cycle the data buffer receives eight new data (in pink) and discard the eight oldest data (in cyan). The newest correlation result (Del + 7) is computed using all the eight newest data.

samples. By taking the correlation values at the correct delay and adding or subtracting the correlation results for each symbol according to the preamble sequence we can reconstruct the full correlation of the received data with the preamble sequence. Moreover, these operations are performed in parallel to produce eight correlation values per 125 MHz clock cycle. The correlation values are compared with a threshold value that can be set manually or automaticaly. The manual threshold can be set by the user using the host PC application. When the threshold is set automatically, the FPGA continuously analyze the correlation values to evaluate their standard deviation and average. The value of the automatic threshold is k times the value of the standard deviation on top of the average (e.g. k = 8). When the threshold is overcome, we save the received data into a fifo together with the value of the TOA counter. The saved data and TOA are sent to the ARM processor to refine the TOA computation and to recognize the tag ID associated to the transmitted sequence.

B. ARM Processing

In Figure 11, the block diagram of the ARM processing to retrieve the tag ID and to refine the evaluation of the TOA is shown. The data buffer transferred from the FPGA to the ARM processor contains a single preamble and tag ID sequence. The exact delay of the preamble sequence inside the buffer varies in the period range of 8 ns.

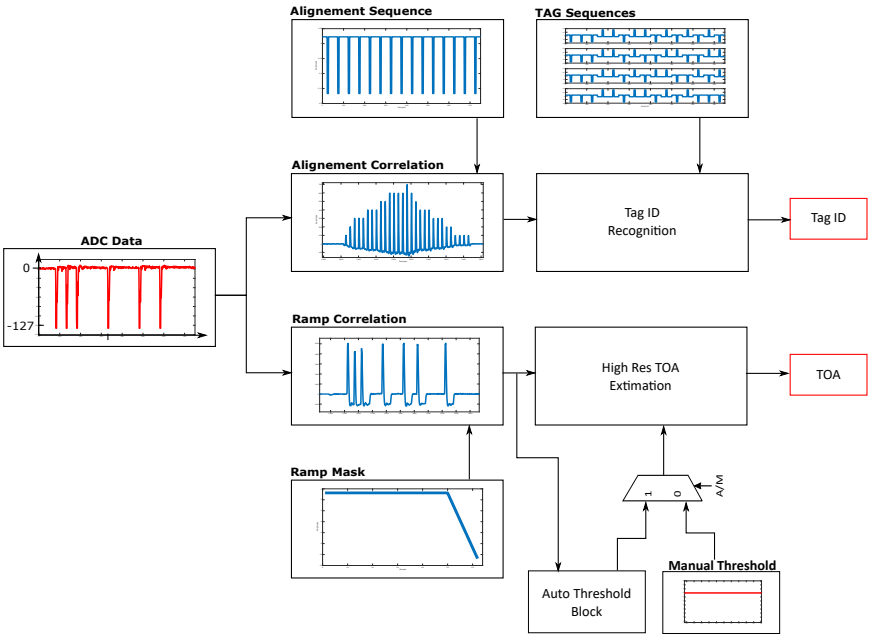

Fig. 11. High level block diagram of the processing steps performed in the ARM processor. The data are elaborated to recognize the tag ID and to refine the TOA estimation with an accuracy of one sample.

In order to locate the start of the tag sequence in the data buffer, we correlate the data with a mask shaped as a sequence of 15 ones (see Figure 11). This correlation is used to align the start of the ID bits and does not requires the maximum achievable accuracy. In this way we can then correlate only the necessary samples reducing the number of computations by almost a factor 2.

To identify the tag associated to the received data we need to correlate them with all the possible receivable tag sequences. The result of this operation is a marker indicating the tag ID corresponding to the transmitting tag. The marker is defined as the maximum correlation value normalized by the number of ones present in the tag ID sequence.

The second part of the information we need to provide is the accurate TOA of the sequence. Since the FPGA processing clock works at a frequency eight times smaller than the sampling one and elaborate the incoming data in parallel, we have a roughness of the TOA of eigth samples (equal to 8 ns). The operations performed in the ARM processor allow to refine the coarse TOA received from the FPGA down to the sampling period of 1 ns (or the upsampling period in case superresolution is applied).

To refine the measure, we correlate the data received from the FPGA with a mask shaped as a discrete linear ramp function defined as

$$R[i] = \begin{cases} 1 & \text{if } 0 \leq i < 45 \\ -3(j-45) & \text{if } 45 \leq i < 50 \end{cases} \tag{10}$$

where i is the mask sample index. The peculiar characteristic of this mask is to highlight the edge of the first sequence peak allowing to measure the TOA corresponding to the direct signal path and not to the ones associated to multipath. The shape of the ramp mask, as well as the received ADC data and the result of the correlation between the two is shown in Figure 11. The results of this correlation are thresholded in order to establish at which sample we find the first edge.

The threshold mechanism can be chosen between manual and automatic. In the first case, the value of the threshold is statically set by a register; in the second case, for each received sequence the threshold is set to one third of the maximum value of the ramp correlation results. The time delay of the first peak is added to the coarse TOA received from the FPGA refining the measurement to the sample period (equal to 1 ns). The computed tag ID and TOA are sent to a host PC running the localization application.

C. Super Resolution

The accuracy in the evaluation of the Time Of Arrival is limited by the sampling period. In our case with a sampling frequency of 1 GHz, the accuracy is as low as 1 ns, that corresponds to 30 cm in distance. To increase the accuracy we could increase the sampling frequency but this would be extreamely cost inefficient.

We propose a solution based on a super resolution technique. The operations performed to implement the super resolution technique are very time consuming, limiting the maximum SRF of tags as the number of tags increase. When using the super resolution, each tag must have a lower SRF (with respect to the case without super resolution), otherwise, the number of tags must be reduced.

The super resolution technique implemented on the ARM processor, performs three main operations:

- Oversampling and linear interpolation;
- Data alignment;
- Averaging.

After the tag ID recognition, each data block is stored in a matrix where, for each tag, the last N (e.g. N = 8) received sequences are saved. The first operation is to oversample by a factor M (e.g. M = 2) the data block and compute the new samples by linear interpolation.
The data alignement operation takes the last received sequence of each tag and correlates it with each one of the previously saved N sequences. This operation allows us to find the relative delay of the N previous sequences with respect to the last received ones. Once the delay among the sequences is known, we align and sum them together. We take advantage of the fact that received sequences close in time do not change their shape dramatically so, by aligning and summing them together, we obtain a better Signal to Noise Ratio.
The obtained upsampled sum is correlated with the ramp mask in order to find the start of the first peak in the same way as we did in the case without super resolution. The oversampling procedure allows to improve the accuracy in the TOA estimation by a number of times equal to the oversampling factor M.

D. PC application and Multilateration Algorithm

The host application receives the data from the sensors and computes the TDOA between the TOA calculated for each signal transmitted by each tag. One of the sensors is chosen as reference and the TDOA are referred to the reference sensor using a reference tag. The obtained TDOA, prior to be used in the trilateration algorithm, are filtered using a median filter and a mean filter. The first filter is used to eliminates the outliers measures that were caused by occlusions between sensors and the tags. The result of the median filtering are then averaged using a mean filter with configurable window.
The TDOA measurements, are used in the multilateration algorithm proposed in [34] to compute the (x,y) coordinates of the tag and plot the results on a 2D map.

V. Results

In this section the results obtained with the system in terms of accuracy, resolution and targets tracking capabilities are shown.
We performed all measurements in a laboratory room 8 m x 8 m. This experimental testbed well represents a realistic indoor harsh environment. The accuracy and resolution tests where performed with the sensors in the same positions indicated in Figure 12. The optimum reference tag position is always close to the center of the area covered by the sensors for optimal reception. In any case, accuracy and resolution are not affected by the relative position of the sensors, tags, and reference tag until the sensors have a good signal reception from each tags. All measurements are taken using three sensors connected through LAN. The preamble sequence is 7 bit long while the tag ID sequence is 8 bit long. The duration of each bit is fixed to 50 ns and contains a single 2 ns UWB pulse at 7.25 GHz. The transmitting SRF is set to 20 Hz. The receiving sampling frequency is 1 Gsps.
The first test intends to verify the localization accuracy: the set up and results are shown in Figure 12. In this first setup, the three sensors are positioned to form a triangular localization area of about 3 m side length. The red, blue and green dots indicates the three sensors positions while the grey dot indicates the reference tag position. A target tag was placed in eigth known positions indicated by the black circles. Each black circle position is ± 60 cm away from the reference tag along the x or y position or both. For each target tag position 256 localization results were collected. The magenta cloud points indicate the positions evaluated enabling the superresolution technique while the blue ones indicate the standard mode of operation. Obviously the position is more accurate when the super resolution technique is enabled; it is also more precise as you can deduce from the point cloud that is significantly smaller.
The accuracy and precision of the localization in the super resoluted case is around to 10 cm.

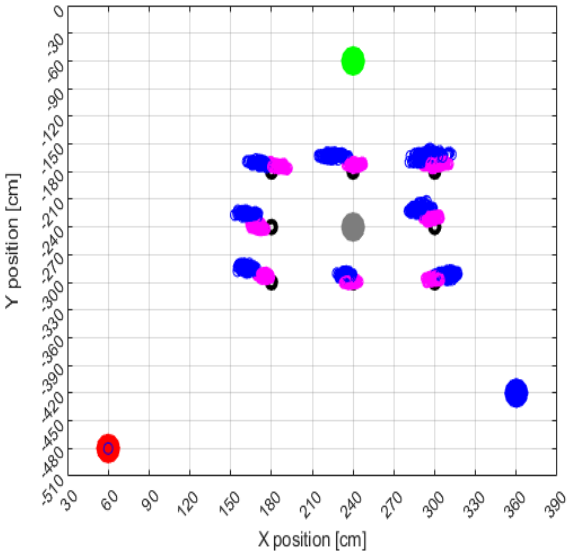

Fig. 12. Ground truth accuracy measurement. The case with super resolution performs better both in accuracy and precision when compared with the standard use case.

To test the resolution we localized two distinct targets placed at different distances using the same setup and enabling the super resolution technique. The results with four different distances are reported in Figure 13 where each plot displays 256 localization results. Starting from the left, the two targets were spaced 60, 40, 20 and 10 centimeters respectively.
In the last case the targets are spaced at the accuracy limit and are still clearly separated. In order to test the tracking capabilities of the system, a kinematic test has been performed without applying the superresolution technique to allow a faster tracking. We attached a target to a rotating structure. During the test we acquired 4096 localization results of the tag rotating at a speed of 6 rotations per minute. The results are shown in Figure 14 and show the continuous track and the very good precision and accuracy obtained demonstrated by the maximum distance of 30 cm between the localization results in red and the ground truth in blue.
To demonstrate the tracking capabilities in a harsh indoor environment, we moved the sensors at the three very corners of

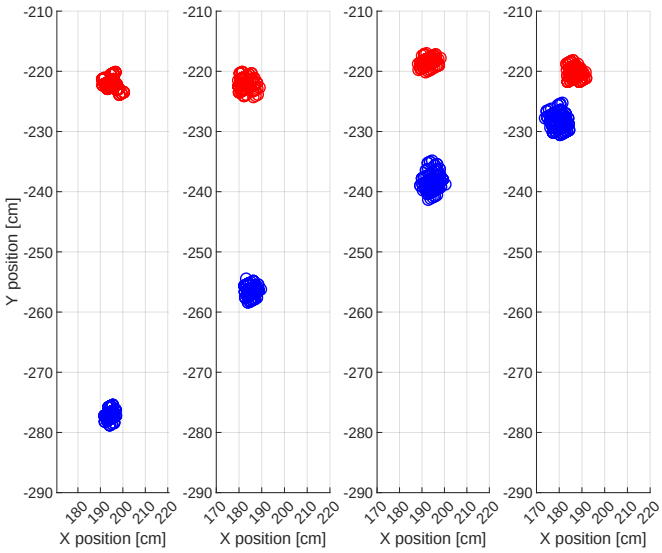

Fig. 13. Resolution measurement using two tags spaced 60, 40, 20 and 10 cm apart and enabling the super resolution.

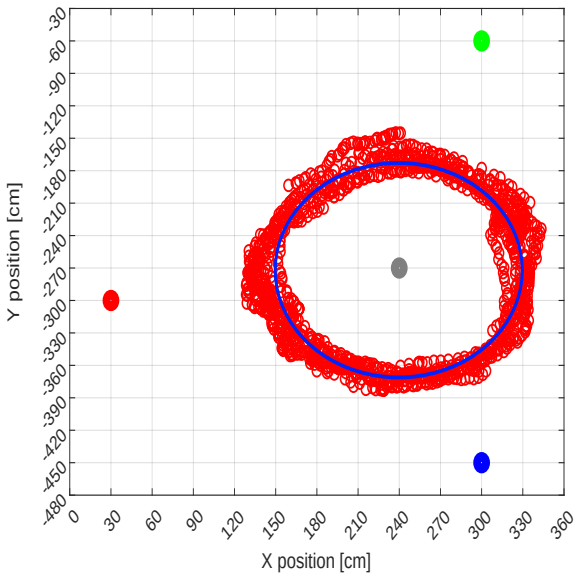

Fig. 14. The tracking measurement results. The red dots represents the 4096 localization results of a single tag rotating around the reference tag while the blue circle is the real track of the tag.

the laboratory room to cover the whole area; the measurements environment is shown in Figure 16. The reference tag is placed at the center of the area covered by the sensors for optimal reception and superresolution technique is not applied. In Figure 15, the blue line represents the track walked by a person carrying the tag, the red dots represents the localization results.

The results show a continuous track and a very good precision and accuracy even when one sensor may be occluded due to the person carrying the tag.

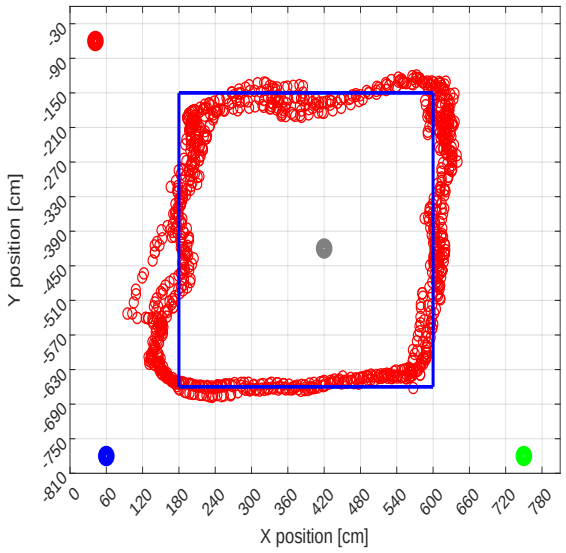

Fig. 15. The tracking measurement results. The sensors are moved further away to cover the whole room area. The blue lines represents the track walked carrying the tag, the red dots represents 1050 localization results.

VI. Conclusions

In this paper, an innovative low-cost UWB real time locating system is presented. For the proposed architecture we designed and manufactured custom hardware and software for both the sensors and the tags.

The system is based on a one way ranging method that significantly reduce the tag and sensor complexity and cost. The use of a reference tag in a fixed position allows to synchronize the sensors, eliminating the need for a common timing reference. We demonstrated the system capabilities to locate tags with 10 cm accuracy and resolution at a typical update rate of 20 Hz by applying superresolution technique in an indoor harsh laboratory environment. We also demonstrated the tracking capabilities of the system.

A comparison based on localization accuracy and implemented localization approach between our system and other solutions already on the market, is presented in table II.

TABLE II
Comparison among UWB RTLS systems

System	Algorithm	Accuracy [cm]
Pulson (P330)	TOA,TDOA,TWR	10
Ubisense	AOA,TDOA	15-20
Zebra	TDOA	30
Sewio	TDOA	30-50
OpenRTLS	TDOA	30
Quantitec	TDOA	15
This work	TDOA	10

Compared to existing solutions, our system is placed among the ones that have the best accuracy performances when the superresolution technique is applied. This demonstrates the reaching of our goal to design and prototype a system architecture with localization accuracy comparable to the existing, more expensive solutions already in the market.

Fig. 16. Indoor laboratory measurement setup. In green, red, blue and gray are highlighted respectively the three sensors and reference tag positions.

A market survey placed the price of all the competitor systems in the order of thousands of USD while our system cost, thanks to the hardware and software custom design, is in the order of hundreds of USD.

REFERENCES

[1] Di Benedetto, M. et al, "Ultra-wideband Communication Systems: A Comprehensive Overview", 1st ed. Wiley (2006).

[2] H. Soganci, S. Gezici and H. V. Poor, "Accurate positioning in ultra-wideband systems," in IEEE Wireless Communications, vol. 18, no. 2, pp. 19-27, April 2011, doi: 10.1109/MWC.2011.5751292.

[3] I. Dotlic, A. Connell, H. Ma, J. Clancy and M. McLaughlin, "Angle of arrival estimation using decawave DW1000 integrated circuits," 2017 14th Workshop on Positioning, Navigation and Communications (WPNC), Bremen, 2017, pp. 1-6;

[4] T. Gigl, G. J. M. Janssen, V. Dizdarevic, K. Witrisal and Z. Irahhauten, "Analysis of a UWB Indoor Positioning System Based on Received Signal Strength," 2007 4th Workshop on Positioning, Navigation and Communication, Hannover, 2007, pp. 97-101, doi: 10.1109/WPNC.2007.353618.

[5] Mazhar, F.; Khan, M.G.; Sällberg, B.; Precise Indoor Positioning Using UWB: A Review of Methods, Algorithms and Implementations. Wireless Pers Commun 97, 4467–4491 (2017).https://doi.org/10.1007/s11277-017-4734-x

[6] Shi G., Ming Y. (2016) Survey of Indoor Positioning Systems Based on Ultra-wideband (UWB) Technology. In: Zeng QA. (eds) Wireless Communications, Networking and Applications. Lecture Notes in Electrical Engineering, vol 348. Springer, New Delhi. https://doi.org/10.1007/978-81-322-2580-5_115.

[7] F. Zafari, A. Gkelias and K. K. Leung, "A Survey of Indoor Localization Systems and Technologies," in IEEE Communications Surveys & Tutorials, vol. 21, no. 3, pp. 2568-2599, thirdquarter 2019, doi: 10.1109/COMST.2019.2911558.

[8] Monica, S.; Bergenti, F. Hybrid Indoor Localization Using WiFi and UWB Technologies. Electronics 2019, 8, 334.

[9] M. Laaraiedh, L. Yu, S. Avrillon and B. Uguen, "Comparison of Hybrid Localization Schemes using RSSI, TOA, and TDOA," 17th European Wireless 2011 - Sustainable Wireless Technologies, Vienna, Austria, 2011, pp. 1-5.

[10] DecaWave RTLS website, available at: https://www.decawave.com/technology1/;

[11] Ubisense RTLS solutions website, available at: https://ubisense.com/

[12] Zebra RTLS website, available at: https://www.zebra.com/

[13] Chantaweesomboon, W.; Suwatthikul, C.; Manatrinon, S.; Athikulwongse, K.; Kaemarungsi, K.; Ranron, R.; Suksompong, P.; (2016). On performance study of UWB real time locating system. 19-24.

[14] Pozyx accurate positioning website, available at https://www.pozyx.io/

[15] Time domain product website, now Humatics. Available at: https://timedomain.com/

[16] Sewio product website, available at: https://www.sewio.net/

[17] Quantitec industrial platform website (IntraNav), available at: https://intranav.com/

[18] OpenRTLS system product website, available at: https://www.airtls.com/

[19] M. Kok, J. D. Hol and T. B. Schön, "Indoor Positioning Using Ultrawideband and Inertial Measurements," in IEEE Transactions on Vehicular Technology, vol. 64, no. 4, pp. 1293-1303, April 2015, doi: 10.1109/TVT.2015.2396640.

[20] S. Sczyslo, J. Schroeder, S. Galler and T. Kaiser, "Hybrid localization using UWB and inertial sensors," 2008 IEEE International Conference on Ultra-Wideband, Hannover, 2008, pp. 89-92, doi: 10.1109/ICUWB.2008.4653423

[21] Corrales Ramon, J.A.; Candelas Herias, F.; Medina, F.; "Hybrid tracking of human operators using IMU/UWB data fusion by a Kalman filter". HRI 2008 - Proceedings of the 3rd ACM/IEEE International Conference on Human-Robot Interaction: Living with Robots. 193-200. 10.1145/1349822.1349848.

[22] Y. Tang, J. Wang and C. Li, "Short-range indoor localization using a hybrid doppler-UWB system," 2017 IEEE MTT-S International Microwave Symposium (IMS), Honolulu, HI, 2017, pp. 1011-1014, doi: 10.1109/MWSYM.2017.8058763.

[23] P. Dabove, V. Di Pietra, M. Piras, A. A. Jabbar and S. A. Kazim, "Indoor positioning using Ultra-wide band (UWB) technologies: Positioning accuracies and sensors' performances," 2018 IEEE/ION Position, Location and Navigation Symposium (PLANS), Monterey, CA, 2018, pp. 175-184, doi: 10.1109/PLANS.2018.8373379.

[24] K. Mimoune, I. Ahriz and J. Guillory, "Evaluation and Improvement of Localization Algorithms Based on UWB Pozyx System," 2019 International Conference on Software, Telecommunications and Computer Networks (SoftCOM), Split, Croatia, 2019, pp. 1-5, doi: 10.23919/SOFTCOM.2019.8903742.

[25] Steggles, Pete and S. Gschwind. "The Ubisense smart space platform." (2005);

[26] A. R. Jiménez Ruiz and F. Seco Granja, "Comparing Ubisense, BeSpoon, and DecaWave UWB Location Systems: Indoor Performance Analysis," in IEEE Transactions on Instrumentation and Measurement, vol. 66, no. 8, pp. 2106-2117, Aug. 2017;

[27] R. Mazraani, M. Saez, L. Govoni and D. Knobloch, "Experimental results of a combined TDOA/TOF technique for UWB based localization systems," 2017 IEEE International Conference on Communications Workshops (ICC Workshops), Paris, 2017, pp. 1043-1048, doi: 10.1109/ICCW.2017.7962796.

[28] M. Kolakowski and V. Djaja-Josko, "TDOA-TWR based positioning algorithm for UWB localization system," 2016 21st International Conference on Microwave, Radar and Wireless Communications (MIKON), Krakow, 2016, pp. 1-4, doi: 10.1109/MIKON.2016.7491981

[29] H. Wymeersch, J. Lien and M. Z. Win, "Cooperative Localization in Wireless Networks," in Proceedings of the IEEE, vol. 97, no. 2, pp. 427-450, Feb. 2009, doi: 10.1109/JPROC.2008.2008853.

[30] H. Matsumoto, H. Kusano, T. Morokuma and K. Sakamura, "Numerical and experimental investigation of TDOA-based positioning system by ultra-wideband impulse radio," 2011 IEEE Topical Conference on

Wireless Sensors and Sensor Networks, Phoenix, AZ, 2011, pp. 25-28, doi: 10.1109/WISNET.2011.5725035.
[31] Laaraiedh, M.; Yu, L;Avrillon, S.; Uguen, B. (2011) Comparison of Hybrid Localization Schemes using RSSI, TOA, and TDOA. 1-5.
[32] T. Gigl, G. J. M. Janssen, V. Dizdarevic, K. Witrisal and Z. Irahhauten, "Analysis of a UWB Indoor Positioning System Based on Received Signal Strength," 2007 4th Workshop on Positioning, Navigation and Communication, Hannover, 2007, pp. 97-101, doi: 10.1109/WPNC.2007.353618.
[33] Tiandong, W.; Xi, C.; Ning, G.; Yukui, P.; "Error analysis and experimental study on indoor UWB TDoA localization with reference tag," 2013 19th Asia-Pacific Conference on Communications (APCC), Denpasar, 2013, pp. 505-508, doi: 10.1109/APCC.2013.6766000.
[34] B.T. Fang, "Simple Solutions for Hyperbolic and Related Position Fixes," *IEEE Trans. Aerosp. Electron. Syst.*, vol. 26, no. 5, Sept. 1990, pp. 748–753
[35] Wikipedia: https://en.wikipedia.org/wiki/Multilateration
[36] "Multilateration (MLAT) Concept of Use", Edition 1, ICAO Asia and Pacific Office, September 2007. Available at: https://www.icao.int/APAC/Documents/edocs/mlat_concept.pdf;
[37] Roslil, S.J., et.al.: "Design of Binary Coded Pulse Trains with Good Autocorrelation Properties for Radar Communications". MATEC Web of Conferences (2018). 150. 06016. 10.1051/matecconf/201815006016.
[38] Alarifi, A.; Al-Salman, A.; Alsaleh, M.; Alnafessah, A.; Al-Hadhrami, S.; Al-Ammar, M.A.; Al-Khalifa, H.S."Ultra Wideband Indoor Positioning Technologies: Analysis and Recent Advances", Sensors 2016, 16, 707.
[39] Macom Low Noise Amplifier product webpage, available at : https://www.macom.com/products/product-detail/MAAL-011130
[40] Minicircuits Bias Tee circuit. Datasheet available at: https://www.minicircuits.com/pdfs/TCBT-14R+.pdf
[41] Lee, Chun-Chi. (2008). An Experimental Study of the Printed-Circuit Elliptic Dipole Antenna with 1.5-16 GHz Bandwidth. Int'l J. of Communications, Network and System Sciences. 01. 295-300. 10.4236/ijcns.2008.14036.
[42] A. Toccafondi, D. Zampilli, C. D. Giovampaola and V. Tesi, "Low-power UWB transmitter for RFID transponder applications," *2012 IEEE International Conference on RFID-Technologies and Applications (RFID-TA)*, Nice, 2012, pp. 234-238.

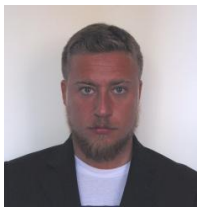

Stefano Bottigliero received the M.Sc. degree in electronic engineering from Politecnico of Torino, Italy, in 2017, where is currently pursuing his Ph.D. His main research interests include localization systems, PCB design for high frequency applications and automotive radar.

Riccardo Maggiora is an Engineer and Professor at Politecnico di Torino, Italy. He has been directing, for more than a decade, the laboratory on radar systems and antennas in his university. He is responsible for the development and implementation of various radar and localization systems for the aerospace, automotive, and industrial sector. He is author of numerous scientific papers.

Daniele Milanesio received a M.Sc. in Computer Engineering at the University of Illinois (Chicago, USA) in 2004; he also graduated in Telecommunication Engineering and received a PhD in Electronics at Politecnico di Torino (Italy), in 2004 and 2008 respectively. He is now associate professor at the Electronics Department of Politecnico di Torino, and member of the laboratory of antennas group. His current research interests are in plasma facing antennas, radar technology and antenna design and measurements.

Maurice Saccani received the M.Sc. degree in electronic engineering from Politecnico of Torino, Italy, in 2009. Since then he is a researcher at Politecnico di Torino, Italy and his main research interests include embedded signal processing for radars and localization systems.